DESIGN AND ANALYSIS OF A COMPACT TENSION (CT) SPECIMEN FOR INTRALAMINAR FRACTURE TOUGHNESS CHARACTERISATION OF WOVEN COMPOSITE LAMINATES

Norbert Blanco[1], Silvestre T. Pinho[2] and Paul Robinson[2]

[1] Analysis and Advanced Materials for Structural Design, Escola Politècnica Superior, University of Girona, E-17071 Girona, Spain
norbert.blanco@udg.edu
[2] The Composites Centre, Dept. of Aeronautics, South Kensington Campus, Imperial College London, SW7 2AZ London, United Kingdom

ABSTRACT

Different specimen geometries for the characterisation of the tensile intralaminar fracture toughness of woven composite laminates have been investigated. The objective is to ensure that the required crack extension for experimental characterisation will occur in the absence of any other damage mechanism. Parametric finite element (FE) analyses in combination with the virtual crack closure technique (VCCT) have been carried out for the different geometries. The specimen geometries analysed were the compact tension (CT) test and four variations of this geometry: extended compact tension (ECT), widened compact tension (WCT), tapered compact tension (TCT) and doubly-tapered compact tension (2TCT). After the results of the parametric analyses, the 2TCT has been considered as the most appropriate specimen geometry for tensile intralaminar fracture toughness characterisation in woven composite laminates. Finally, a series of experimental tests have been carried out in order to validate the parametric analysis. Good agreement has been found between the experimental results and the numerical predictions of the parametric analysis.

1. INTRODUCTION

Final failure of laminated composite structures is preceded by different damage mechanisms involving fracture initiation and propagation. The evaluation of damage onset, fracture propagation mechanisms and associated fracture toughness are important in the design of efficient and durable fibre reinforced composite structures. Fracture in a composite laminate can appear either between two plies or within a lamina. In the first case, interlaminar fracture or delamination, the crack causes separation of two adjacent plies and will mainly involve matrix failure or matrix-to-fibre debonding although some failure of fibres bridging the delamination may also occur. There are numerous studies addressing this subject in the scientific literature. In the second case, intralaminar or translaminar fracture, the crack is located within the lamina, either parallel to the fibres (matrix crack) or at an angle (with fibre failure). When an intralaminar crack propagates at an angle to the reinforcing fibres, the fibres bridge both surfaces of the crack, arresting or reducing further crack opening until the bridging fibres are broken. Intralaminar cracks and measurement of the associated toughness have received less attention in the literature than delamination or interlaminar cracks.

Although the energy consumed in fibre fracture is usually much larger than in matrix cracking or fibre-matrix debonding [1], experimental determination of the fibre fracture toughness is important for accurate numerical modelling of composite component failures. In the literature, there are some studies dealing with the experimental evaluation of the intralaminar fracture toughness of composite laminates involving fibre fracture. In most of the cases, the compact tension (CT) test has been employed. The CT test was initially developed for metallic materials [2] but it has been successfully used to measure the intralaminar fracture toughness of composite laminates that have been

laminated with unidirectional plies. However, experimental evidence has shown that for woven composite laminates different damage mechanisms can occur in addition to, or instead of, the intended intralaminar crack propagation so invalidating the fracture toughness measurement.
The objective of the present investigation is to determine an appropriate test specimen geometry for intralaminar fracture toughness characterisation of woven composite laminates ensuring intralaminar crack propagation in the absence of any other failure mechanism. In addition to the CT specimen geometry, four different variants of this have been considered in the study. A series of parametric analyses has been carried out to determine the influence of different geometric parameters on the failure mechanisms. As a result, a modified fracture specimen has been designed for intralaminar fracture toughness characterisation of a woven composite laminate ensuring crack propagation before the occurrence of any other failure mechanism. The study is completed with the experimental characterisation of the intralaminar fracture toughness of a woven composite laminate using the designed specimen geometry. Good agreement has been found between the experimental results and the predictions of the parametric analysis.

2. PARAMETRIC ANALYSIS OF THE FRACTURE SPECIMENS

Parametric analyses of five different fracture specimens have been carried out by means of the finite element method (FE) in combination with the virtual crack closure technique (VCCT). The parametric study has included linear and nonlinear elastic analyses to take into account different damage mechanisms, as well as the out-of-plane displacement of the specimen due to overall specimen buckling. In the linear analyses, symmetry was employed and only one half of the specimen was modelled.

2.1 Material properties

The material considered for the analyses was the 5HS-RTM6 0-90° woven composite. This is a Tenax five-harness satin carbon fibre fabric with an epoxy Hexcel RTM 6 resin. The in-plane mechanical properties of the material are summarised in Table 1 [3], where subscript t stands for tension, subscript c for compression and superscript u for ultimate strength. The nominal thickness of the ply is 0.35 mm and the reference stacking sequence considered in the study for the static analyses has been $[0\text{-}90]_{4s}$, where 0-90 stands for the principal directions of one layer (warp and fill, respectively). However, in order to take into account the effect of the thickness of the specimen during buckling analyses, the $[0\text{-}90]_{2s}$ and $[0\text{-}90]_{8s}$ stacking sequences have also been considered. Therefore, the thickness of the specimens considered for the linear analyses has been t = 2.8 mm, whilst for the classical buckling analysis the thicknesses considered have been t = 1.4, 2.8 and 5.6 mm.

Table 1: Mechanical properties of the 5HS-RTM6 carbon fibre composite [3] (x-direction corresponds to the fill direction and y-direction to the warp direction).

E_{xx} (MPa)	E_{yy} (MPa)	G_{xy} (MPa)	ν_{xy}	X_t^u (MPa)	X_c^u (MPa)	Y_t^u (MPa)	Y_c^u (MPa)	S^u (MPa)
66537	68467	4571	0.04	807	657	848	689	103

2.2 Geometry of the fracture specimens

In total, five different fracture specimens have been considered, namely the compact tension (CT) which is shown in Figure 1(a), the extended compact tension (ECT), the widened compact tension (WCT), the tapered compact tension (TCT) and the doubly-tapered compact tension (2TCT) which is shown in Figure 1(b). The ECT specimen is

an elongated version of the CT specimen in which the height of the specimen is incremented while the rest of the geometry is kept constant. This has been standardised by ASTM for the fracture toughness characterisation of composite laminates [4]. The WCT specimen is a widened version of the CT specimen where the width of the specimen has been doubled while the rest of the geometric parameters remain constant. The TCT specimen is a version of the CT specimen where the height of the specimen is tapered towards the right hand edge as indicated in Figure 1(b). The 2TCT specimen is a modification of the TCT specimen in which the height of the specimen is tapered towards both the left and right edges of the specimen as shown in Figure 1(b).
The geometric parameters considered in the analyses, see Figure 1(a), were the height h of the specimen, the width w of the specimen, and the horizontal and vertical locations of the loading holes, x and e respectively, as well as the crack length a. For the TCT and 2TCT specimens, also the horizontal and vertical dimensions of the taper, f and g, were considered. Also in these specimens, the height of the specimen between the tapered zones is defined by h while the total height of the specimen is h_1.

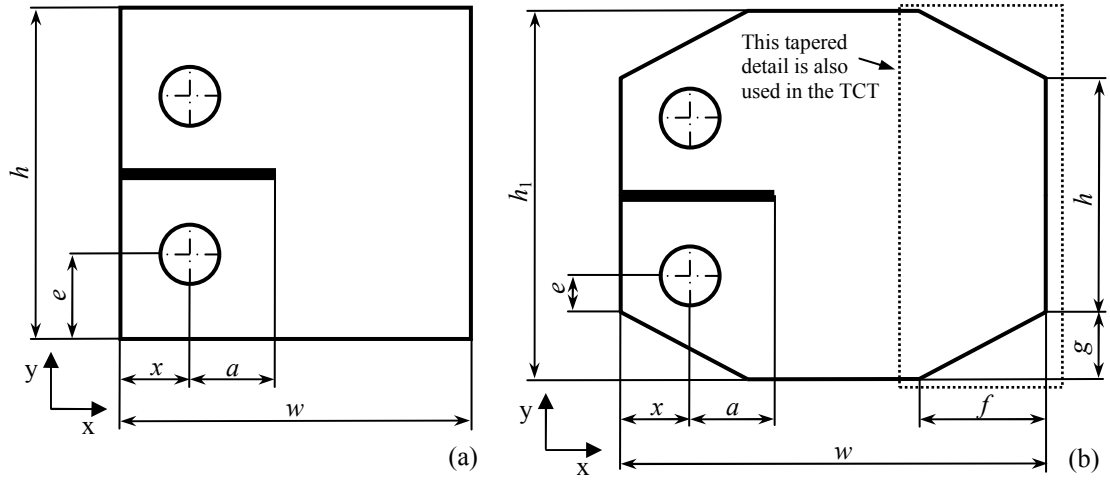

Figure 1: Schema of the (a) CT and (b) 2TCT fracture specimens with the geometric parameters considered in the parametric analysis (Note: dimensions f and g are identical for all tapered regions).

During the parametric analysis, for every geometry type a reference specimen has been defined and only one of the geometric parameters has been varied at a time, except for a, to investigate its influence on the different damage mechanisms. For the CT specimen the reference values are w = 65 mm, h = 60 mm, x = 14 mm and e = 16 mm with a = 30 mm. This geometry is compliant with the ASTM E399-90 standard [2]. For the ECT specimen, the reference specimen is defined by w = 65 mm, h = 240 mm, x = 14 mm, e = 23 mm and a = 30 mm, which results in a geometry compliant with the ASTM E1992-04 standard. The WCT reference specimen has been defined with w = 130 mm, h = 60 mm, x = 14 mm, e = 16 mm and a = 30 mm. Finally, the reference values for the TCT and 2TCT specimens have been set to w = 85 mm, h = 44 mm, x = 14 mm, e = 7 mm, f = 25 mm, g = 20 mm and a = 30 mm. In all cases, it has been assumed that the x-direction of the specimen corresponds to the fill direction of the fabric and the y-direction corresponds to the warp direction (see Figure 1(a)).

2.3 Failure mechanisms

The damage mechanisms and associated failure mechanisms taken into account in this study include some of those reported by Minnetyan and Chamis for the CT specimen

[5] as well as buckling. The locations of the potential failures are labelled FM_i in Figure 2 and the corresponding failure mechanisms considered were as follows.
i = 1: fibre fracture due to longitudinal compressive stress σ_{yy} at the right edge;
i = 2: fibre fracture due to longitudinal compressive stress σ_{xx} at upper and lower edges;
i = 3: matrix cracking due in-plane shear stress σ_{xy};
i = 4: bearing in the holes of the specimen due to compressive stress;
i = 5: shear-out in the holes of the specimen due to shear stress and
i = 6: overall specimen buckling.

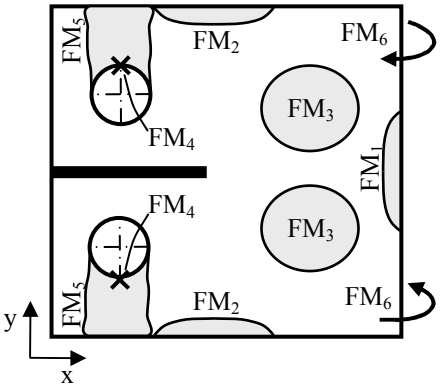

Figure 2: Schema of the CT specimen and location of the failure mechanisms.

Each failure mechanism is predicted using a corresponding failure index defined in Table 2. The stresses and forces indicated in the table correspond to an applied load such that the energy release rate at the crack tip reaches a critical value. Regarding the strengths used in failure indices 1 and 2, an earlier work by Osada et al. [6] pointed out that nonlinear behaviour for a 4-harness satin composite laminate was identified at 37 % of ultimate strength when the composite was tested under unidirectional stress in the warp direction. This nonlinear behaviour was associated to transverse matrix cracking in the fill fibre bundles followed by fibre fracture in the warp bundles. Thus, in this work a conservative factor of 3 has been considered and the following strengths, accordingly to the onset of matrix cracking, have been defined: $X_c = X_c^u/3$ and $Y_c = Y_c^u/3$.
FE simulations were carried out with a unit load P = 1 applied to the specimen, from which the corresponding stresses σ and energy release rate G were obtained. Given the linear behaviour, the load P_c such that the energy release rate at the crack tip reaches a critical value, and the corresponding stress σ_c in the specimen, are given by

$$P_c = P\sqrt{\frac{G_{Ic}}{G}} \qquad \sigma_c = \sigma\sqrt{\frac{G_{Ic}}{G}} \qquad \text{(1(a) \& (b))}$$

where G_{Ic} is the laminate mode I fracture toughness for the fibre failure mode, which has been estimated here as 100 kJ/m^2 [2]. Using Eqs. 1(a) and (b), the failure indices in Table 2 can be calculated, where σ_{xxc}, σ_{yyc} and σ_{xyc}, are the critical x- and y-direction direct and shear stresses, respectively, X_c is the compressive strength of the material in the fill direction, Y_c is the compressive strength of the material in the warp direction, S is the in-plane shear strength of the material, P_b the applied load to generate buckling in the specimen and d is the diameter of the loading holes.

Table 2: Failure indices corresponding to the failure mechanisms indicated in Figure 2.

Failure mechanism	FM_1	FM_2	FM_3	FM_4	FM_5	FM_6
Failure index (FI)	$\frac{\sigma_{yyc}}{Y_c}$	$\frac{\sigma_{xxc}}{X_c}$	$\frac{\sigma_{xyc}}{S}$	$\frac{P_c}{t \cdot d \cdot Y_c}$	$\frac{\frac{3}{2}P_c}{2 \cdot t \cdot e \cdot S}$	$\frac{P_c}{P_b}$

2.4 Results of the parametric analysis and discussion

Figure 3 shows typical FE results obtained during the parametric analysis of the CT specimen. It can be observed that apart from the expected stress concentrations around the crack-tip, the linear FE simulations predict high compressive σ_{xx} stresses at the upper and lower edges of the specimen, high compressive σ_{yy} stresses at the right edge and σ_{xy} stress concentrations between the crack-tip and the end of the specimen. It can be also seen that the nonlinear FE simulations predict a buckling mode where the back of the specimen twists forcing the upper and lower corners at the right edge to move in opposite ways in the out-of-plane direction. The stress concentrations and the out-of-plane displacements for the ECT, WCT, TCT and 2TCT specimens are similar to those shown in Figure 3.

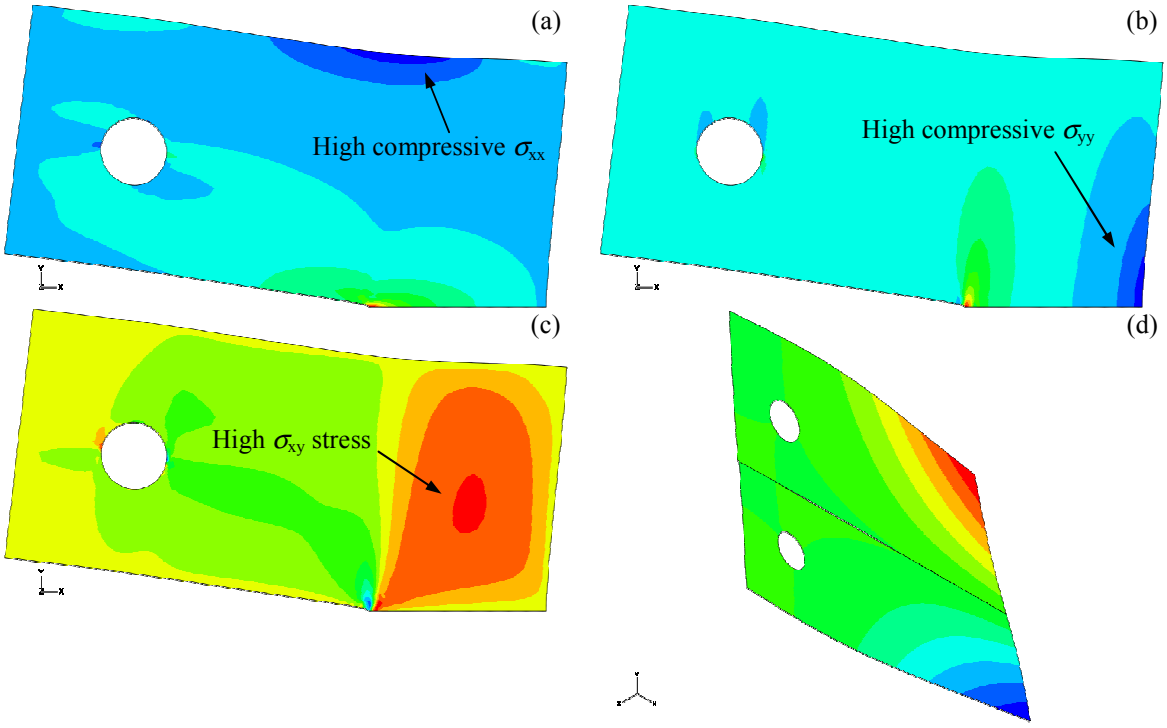

Figure 3: Finite element results for the reference CT specimen when a = 30 mm: (a) σ_{xx}, (b) σ_{yy}, (c) σ_{xy} stress distributions and (d) out-of-plane displacements in buckled state.

The results of the parametric analysis for the CT specimen when only one of the geometric parameters is varied at a time are shown in Figure 4. In the figures, the horizontal axis represents the value of the geometric parameters expressed as a percentage of the reference value. It can be observed in the figure that the most critical failure indices are FI_1 and FI_2. In particular, FI_1 can achieve values higher than 5 for the range of parameters considered. This indicates that the CT specimen would exhibit extensive matrix cracking and fibre fractures at the right edge of the specimen due to longitudinal compressive stress σ_{yy} and eventually fail before crack extension. It can be also observed that FI_1 increases with the crack length.

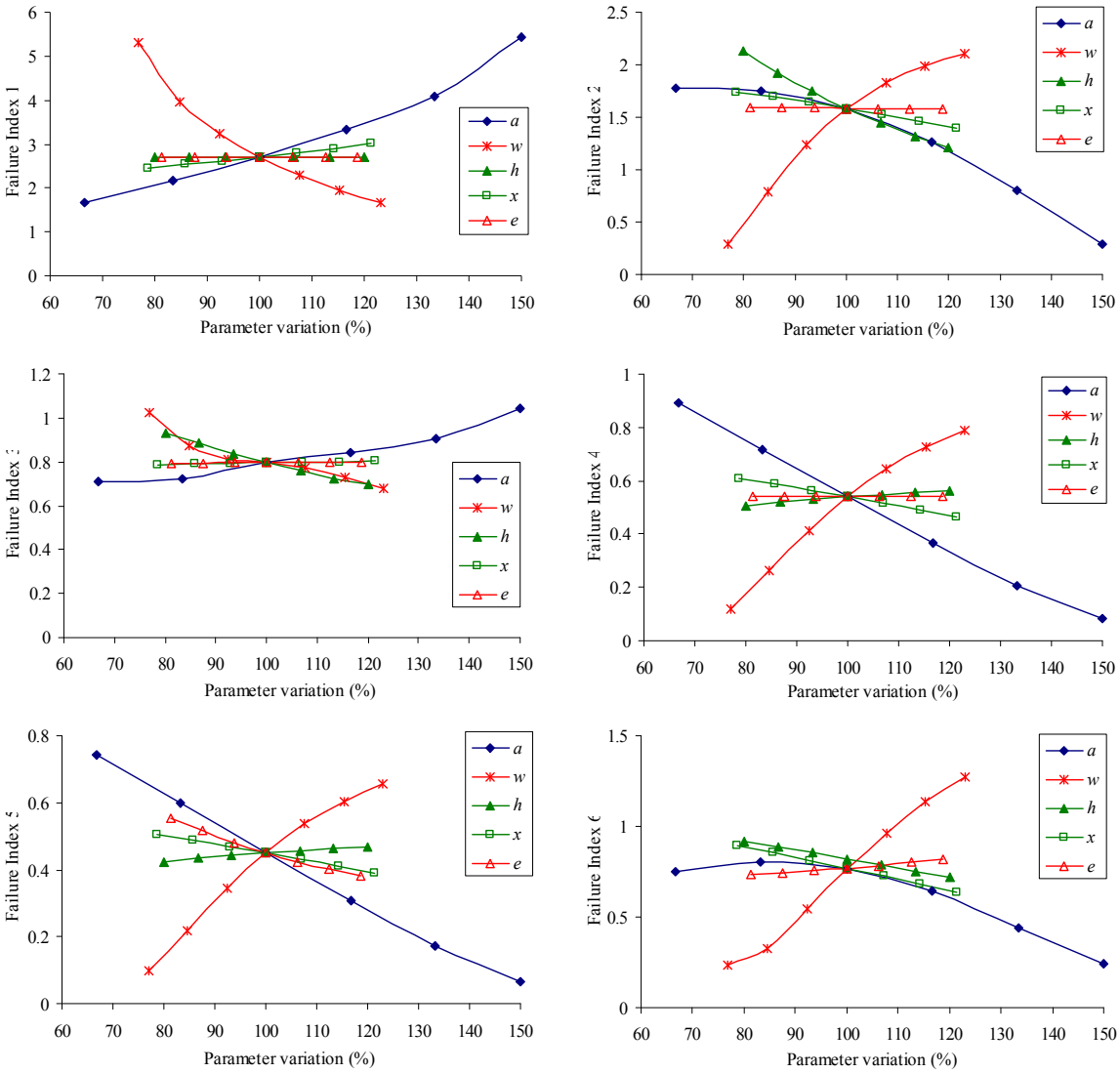

Figure 4: Variation of the failure indices for the CT specimen.

The results presented in Figure 4 show that the parameters that have greatest influence on FI_1 and FI_2, apart from crack length, are the *w* and *h*; the rest of the parameters have a relatively minor influence. Observing the variation of the failure index FI_1 with *w*, it can be concluded that the compressive stress at the right edge of the specimen can be reduced by increasing *w*. However, higher values of *w* result in higher values of the rest of the failure indices except for FI_3. Actually, this is in good agreement with the results obtained for the WCT specimen in which FI_1 is lower than 1. In this case, all the failure indices increase in comparison to the CT specimen except FI_1 and FI_3, and the highest indices are FI_2 and FI_6 which reach maximum values of 2.9 and 2.4 respectively.
On the other hand, the variation of *h* has no effect on FI_1 but a considerable reduction of FI_2 and FI_3 can be achieved by increasing *h*. On the rest of the failure indices, *h* has little effect. This is in very good agreement with the results obtained in the parametric analyses of the ECT specimen. Actually, for the ECT specimen and the range of parameters considered, the variation of FI_1 is similar to that of the CT specimen except that the influence of *w* is lower, FI_2 is reduced to one tenth and FI_6 is increased.
Figure 5 presents the resulting variations of the three most critical failure indices (FI_1, FI_2 and FI_6) for the TCT and 2TCT specimens. The variations of the other three failure

indices are similar to those of the CT specimen. For TCT and 2TCT specimens, x and e have not been varied as their effect on the failure indices is very low.

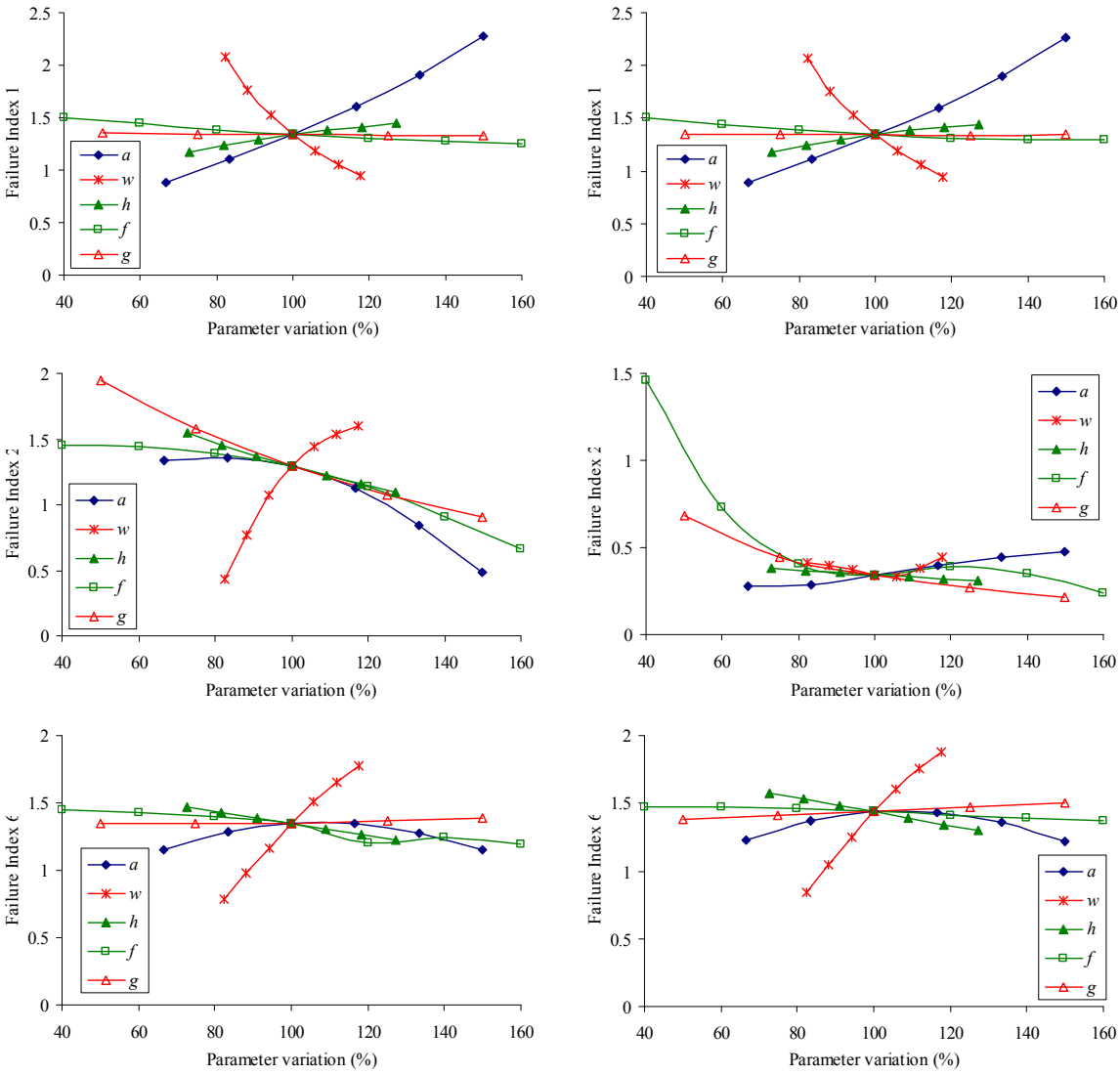

Figure 5: Variation of the most critical failure indices for the TCT (left) and 2TCT (right) specimens.

From Figure 5, it can be seen that the variation of FI_1 is the same for the TCT and 2TCT specimens with values lower than half those of the CT and ECT specimens. A similar situation is encountered for FI_6, although in this case the obtained values are higher than those for the CT and ECT specimens. Finally, the values for FI_2 are lower in the case of 2TCT specimen. Actually, lower values of FI_2 can be only achieved with the ECT specimen. Thus, the 2TCT specimen can be seen as the fracture specimen that achieves generally lower values for the failure indices.

In conclusion, although none of the specimen geometries were able to achieve values for all the failure indices of less than one, the doubly-tapered compact tension (2TCT) specimen seems to be the most suitable geometry for tensile intralaminar fracture toughness characterisation of woven composite laminates. For the experimental characterisation of the intralaminar fracture toughness of the carbon/epoxy 5HS-RTM6, described in the next section, a 2TCT specimen with the following dimensions was chosen: w = 90 mm, h = 40 mm, x = 14 mm, e = 7 mm, f = 20 mm, g = 15 mm and a

nominal thickness t = 5.6 mm. For this geometry, the predicted variation of the failure indices with the crack length can be seen in Figure 6. Most of the failure indices are under or very close to the unity for the considered range of crack length. Only FI_1 is critical, although its maximum value does not reach two. Considering that a conservative factor of one third has been applied to the strength used to define the failure indices, it can be assumed that only for very long crack lengths will damage mechanisms other than crack propagation occur in the specimen.

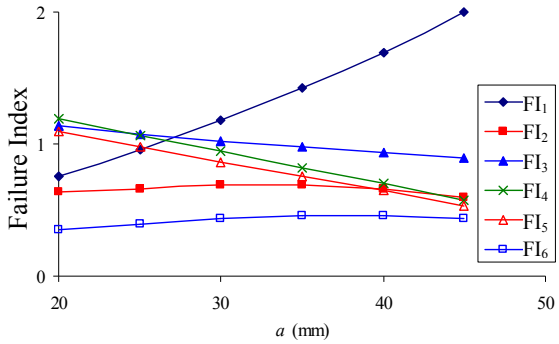

Figure 6: Variation of the critical failure indices as a function of the crack length for the experimental 2TCT specimen.

2.4 Data reduction

Following a similar procedure to Pinho et al. [1], the critical energy release rate of the laminate in mode I can be evaluated for the designed 2TCT specimen as a function of the applied load and the crack length as:

$$G_{\text{Ic-lam}} = \left(\frac{P_c}{t}\right)\left(c_3 a^3 + c_2 a^2 + c_1 a + c_0\right) \qquad (2)$$

in which P_c is the experimental load associated with crack propagation at crack length a and the coefficients c_i, given in Table 3, have been determined from FE analyses.

Table 3: Coefficients for the interpolation of $G_{\text{Ic-lam}}$ as a function of the crack length.

Crack length	c_3	c_2	c_1	c_0	error (%)
$19 \le a < 30$ mm	1.36×10^{-9}	-6.39×10^{-8}	1.88×10^{-6}	-1.95×10^{-6}	< 0.01
$30 \le a < 40$ mm	5.44×10^{-9}	-4.50×10^{-7}	1.41×10^{-5}	-1.31×10^{-4}	< 0.01
$40 \le a < 50$ mm	2.90×10^{-8}	-3.38×10^{-6}	1.36×10^{-4}	-1.82×10^{-3}	< 0.01
$50 \le a < 60$ mm	2.81×10^{-7}	-4.27×10^{-5}	2.19×10^{-3}	-3.74×10^{-2}	< 0.01
$60 \le a < 65$ mm	4.01×10^{-6}	-7.19×10^{-4}	4.32×10^{-2}	-8.65×10^{-1}	< 0.01

3. EXPERIMENTAL CHARACTERISATION OF THE INTRALAMINAR FRACTURE TOUGHNESS

3.1 Experimental procedure

The tensile intralaminar fracture toughness of the carbon/epoxy 5HS-RTM6 woven composite material has been experimentally characterised using the 2TCT test. In total, six specimens with the previously defined geometry were tested, all of them with a $[0\text{-}90]_{8s}$ stacking sequence, with a nominal thickness t = 5.6 mm.

Before testing, all the specimens were cut with a wet diamond saw and the dimensions of each specimen were measured. The 8 mm diameter holes were drilled holding the specimen in between two sacrificial pieces of similar composite. To ensure a sharp crack tip for the pre-crack, first an approximate 29 mm long notch was cut with a diamond saw. Then, three 0.2 mm thick razor saws with 32, 42 and 52 razor teeth per

inch were used one after another to obtain a thin and sharp 5 mm extension of the pre-crack. Finally, a 0.1 mm thick razor blade was used to further sharpen the crack tip using a sawing action. A speckle pattern was created on one face of each specimen using white ink spray for use with a digital image correlation (DIC) system (Aramis) to enable specimen displacements and strains to be monitored during a test (although the contrast is not as high as painting the specimens white and using a black speckle pattern, the latter approach has been observed to lead to peeling of the background paint, making crack measurement difficult and preventing DIC from returning valuable data corresponding to the peeled region [1]). Finally, a 1 mm increment scale was drawn onto each specimen to monitor the crack length propagation during the test. All the tests were carried out under displacement control at a rate of 0.5 mm/min in an Instron testing machine with a 15 kN load cell. A CCD camera was used to view a magnified image of the crack-growth scale in combination with an event-marker connected to the data logger. The DIC system was positioned to examine the surface of the specimen recording the strain field in the specimen to check for damage not readily visible with the CCD camera or naked eye.

3.2 Experimental results and discussion

No problems arose during the tests and no apparent damage other than crack propagation could be seen. As expected, the crack growth observed during the test of the six specimens presented several crack jumps of a few millimetres each, Figure 7(a). The R-curves (i.e. G_{Ic} versus a) obtained from the six specimens are summarised in Figure 7(b). The average critical energy release rate is ~ 62 kJ/m^2 with a standard deviation of 10 %.

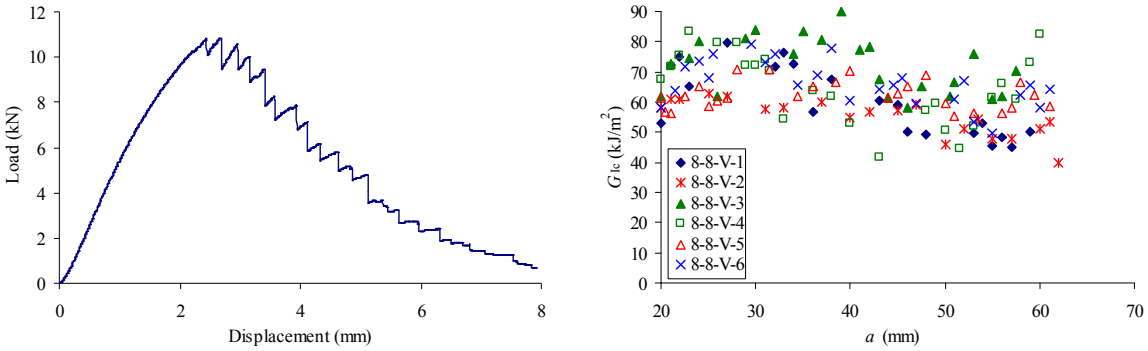

Figure 7: Typical load vs. displacement curve for the 2TCT specimen (left) and R-curves for the six 2TCT specimens (right).

As mentioned, during the tests no other damage mechanism other than crack propagation could be observed in the specimens. This was confirmed monitoring the specimens after the tests by the strain fields determined from DIC, and C-scan and X-ray images. Figure 8(b) shows a DIC image of a tested specimen in which only the damage generated by crack propagation is observed. Figures 8(c) and (d) show the C-scan and X-ray images of the same specimen where it can be seen that in the interior of the specimen there is no damage in the fibres or matrix away from the zone of the propagation of the crack.

4. CONCLUSIONS

Parametric analyses of the CT, ECT, WCT, TCT and 2TCT specimens have been carried out to determine the most appropriate fracture specimen for intralaminar fracture

toughness characterisation in woven composite laminates. Different failure indices have been defined to ensure crack propagation without the occurrence of any other damage mechanism and it has been concluded that the 2TCT is the most appropriate specimen. This specimen has been successfully used to experimentally characterise the intralaminar fracture toughness of a woven composite laminate.

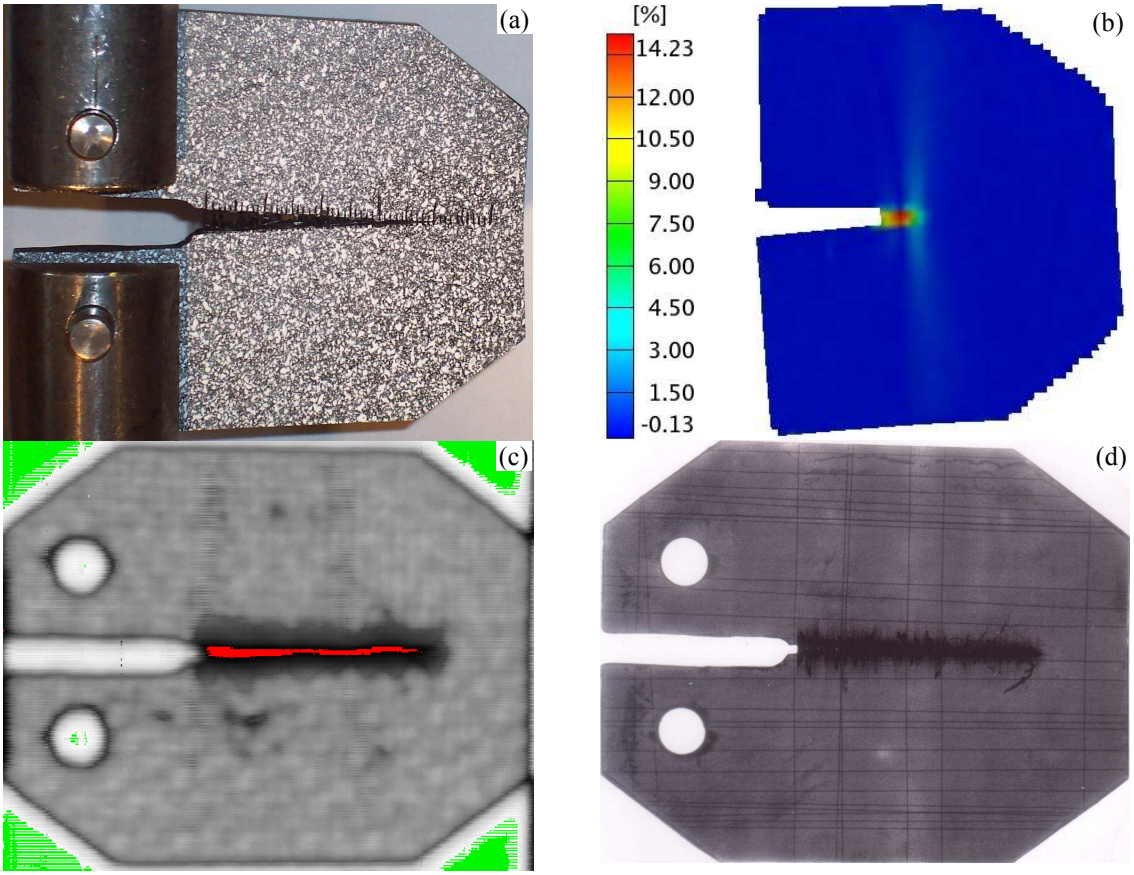

Figure 8: 2TCT (a) photograph during testing, (b) DIC image at a stage during testing showing the major strain and (c) C-scan and (d) X-ray images after testing.

ACKNOWLEDGEMENTS

The first author would like to acknowledge financial support from the Spanish Government under research project MAT2006-14159-C02-01.

REFERENCES

1- Pinho, S.T., Robinson, P., Iannucci, L., "Fracture toughness of the tensile and compressive fibre failure modes in laminated composites", *Composites Science and Technology*, 2006; 66(13): 2069-2079.
2- ASTM E399-90, "Standard test method for plain-strain fracture toughness of metallic materials", 2003; 427-528.
3- Campbell, K., "Material characterisation – 5HS/RTM6", Bombardier Aerospace (internal report), 2004.
4- ASTM E1922-04, "Standard test method for translaminar fracture toughness of laminated and pultruded polymer matrix composite materials", 2003; 1159-1163.
5- Minnetyan, L., Chamis, C.C., "The C(T) specimen in laminated composite testing", *NASA Technical Memorandum 4712*, 1996.
6- Osada, T., Nakai, A., Hamada, H., "Initial fracture behaviour of stain woven fabric composites", *Composites Structures*, 2003; 61(4): 333-339.